IEEE Access
Multidisciplinary | Rapid Review | Open Access Journal

Received May 31, 2020, accepted June 17, 2020, date of publication June 22, 2020, date of current version July 2, 2020.

Digital Object Identifier 10.1109/ACCESS.2020.3003949

Optimal PV-INV Capacity Ratio for Residential Smart Inverters Operating Under Different Control Modes

TAHA SELIM USTUN[1,2], (Member, IEEE), YUKI AOTO[1], JUN HASHIMOTO[1,2], AND KENJI OTANI[1,2]

[1]Fukushima Renewable Energy Institute, AIST, (FREA), Koriyama 963-0298, Japan
[2]Department of Energy and Environment, Research Institute of Energy Frontier, Tsukuba 305-8589, Japan

Corresponding author: Yuki Aoto (yuki.aoto@aist.go.jp)

This work was supported by the Ministry of Energy, Transportation and Industry, METI, Japan.

ABSTRACT The ratio between the photovoltaic (PV) array capacity and that of the inverter (INV), PV-INV ratio, is an important parameter that effects the sizing and profitability of a PV project. It is important to find the balance between cutting down costs by under-sizing the inverter and maximizing profits by generating more energy. This becomes much more important where smart inverters with voltage control abilities are utilized. Smart Inverters have the ability to actively take part in voltage control and, thus, increase the injected power. This would require a larger capacity than usual, as some reactive power flow needs to be accommodated to limit the voltage rise. Excess capacity can be utilized to implement smart inverter functionalities and inject more energy under conditions where conventional inverters would cap their generation. Furthermore, PV-INV ratio studies in the literature focus on large-scale, grid-connected PV systems. This paper focuses on investigating PV-INV ratio for residential PV systems with smart inverters. These are connected to low-voltage distribution systems where voltage rise issue is more apparent. A new simulation tool that can model smart inverter functionalities is utilized to investigate the impact of PV-INV ratio on overall power generation. Different smart inverter functions are implemented for comparison. Based on simulation results, the overall costs and power generation are documented for different PV-INV ratios. Finally, a cost-benefit analysis is performed to find out which PV-INV ratio yields the maximum profits with minimum costs.

INDEX TERMS Smart inverters, distributed control, distribution grid dynamics, power system modeling, active distribution networks, optimal sizing of smart inverters.

I. INTRODUCTION

Novel issues in grid control and operation appear with increasing renewable energy penetration levels [1]. Engineers, environmentalist and politicians are all looking at solutions that lead to mode deployment of renewables [2]. New approaches and systems are required to achieve this objective [3], [4]. Most of the renewables are connected to the grid with inverters and this creates inertia issues that relate to voltage and frequency stability. Smart Inverters (SIs) are utilized to mitigate these unwanted effects of renewables on the grid [5]. Unlike their conventional counterparts, SIs can operate in entire P-Q plane. SIs have the ability to absorb and inject real and reactive power. This advanced capability has many unknowns and more studies are required to understand their behavior better [6].

Electric power companies are reluctant to adopt new technologies, especially, when, there are many unknowns. It is also true that proven technologies with quantifiable benefits are rapidly integrated into their systems, such as use of Flexible AC Transmission Systems (FACTS) instead of building new transmission lines [7]. Likewise, SIs may bring real benefits to power system operation, in terms of increased auxiliary support on voltage and frequency. With these supports SIs may help grid operators meet their renewable energy targets without doing substantial changes to the grid [8]. However, it is imperative to study their impacts before going into mass deployment.

The associate editor coordinating the review of this manuscript and approving it for publication was Siqi Bu.

Despite being new, SIs have received a lot of attention in the literature such as comparing their operating modes [9], developing new ones [10] or tackling changing weather conditions [11]. Most of these studies focus on SIs that are connected to high-voltage networks, such as solar farms. However, the real voltage disturbances are observed in distribution networks that are designed to operate as passive networks. Therefore, there is an immediate need to study SI impact on low-voltage distribution networks.

Furthermore, all of these works focus on the immediate impact of SIs on voltage regulation or frequency control. There is need for a research that looks at the long-term of SIs with their functionalities, how they increase the locally generated power, and the revenue. It is important to understand the nature in which SIs impact the amount of captured renewable energy over a period of time and how the voltage-limitation is mitigated so that renewable energy capping is avoided. These two phenomena should be understood well to find the optimum point between having a very expensive SI with a high capacity and a small SI that generates less energy but costs much less.

In this paper, the impact of the ratio between PV panel capacity and inverter capacity on overall generation and system financing has been studied. A novel simulation tool is developed to integrate SIs into the power flow. Real solar radiation measurements collected on site are utilized along with realistic load profiles. Simulations are run with conventional inverters (i.e. no smart functions) as well as different smart inverter functionalities. Annual generation amount is calculated when over-voltage rules are applied as per the grid code. Cash flow analysis is performed to calculate total profit and payback period for a typical lifetime of a PV system, i.e. 25 years. Results are compared to evaluate the impact of smart inverter on grid operation, overall generation and financing of such projects. Fair use of the distribution network is a rising concern among residential PV owners as the physical location of a PV system stipulates how much power can be sold to the grid. The results are analyzed for fair-use and several recommendations are given.

The rest of the paper is organized as follows. Section 2 gives an overview of SIs and their abilities. Sections 3 and 4 detail the mathematical problem modeling and the new simulation tool that is utilized to run power flow studies with SIs. Section 5 presents the simulation parameters such as network model, load and solar radiation profiles as well as employed smart inverter controls. Simulation results and their impact on the overall generated power and payback period are given in Section 6. Section 7 draws the conclusions and gives research directions for futurework.

II. OVERVIEW OF SMART INVERTERS AND THEIR CAPABILITIES

IEC/TR 61850-90-7 is the main document that lists the operating modes of SIs and defines their working principles [5]. As shown in Table 1, there are several modes grouped under seven main classes. The most important ones are those listed in second and third classes, as they actively contribute to voltage and frequency control in the grid.

TABLE 1. Smart inverter capabilities listed in IEC61850-90-7.

Modes	Functions
Immediate Control	INV1: grid connect/disconnect
	INV2: adjust max. generation level up/down
	INV3: adjust power factor
	INV4: request active power
	INV5: Pricing signal (charge/disch.)
Volt-Var Management	VV1: Available Var support, no P impact
	VV2: Max. Var support based on Wmax
	VV3: Static Power Converter
	VV4: Passive Mode (No Var support)
Frequency Related	FW21: High freq. reduces P
	FW22: Limiting generation with f
Dynamic Reactive Current Support	TV31: Support during abnormally high or low voltage
Low-high voltage ride-through	"Must disconnect" (MD) "Must remain connected" (MRC)
Watt triggered	WP41: Watt power factor
	WP42: Alternative watt power factor
Volt-watt management	VW51: Volt-Watt management (generation)
	VW52: Volt-Watt management (charging)
Non-power parameters	TMP: temperature
	PS: pricing signal
Setting and Reporting	DS91: Modify DER settings (power conv.)
	DS92: Log alarms and events
	DS93: Selecting status points
	DS94: Time synchronization requirements

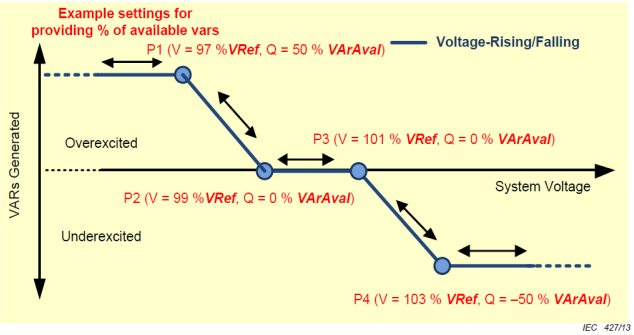

FIGURE 1. VV11 var support mode control curve without hysteresis.

Volt-var control modes hold a very important point for distributed renewable energy generation. The reason is that local power injection to the distribution grid causes voltage rise problems and limits the amount of captured energy. VV1 mode, called PQ control in this paper, can be utilized to exchange reactive power Q to control voltage rise and continue real power P injection. As shown in Figure 1, reactive power Q can be sourced and received by the SI to help with stabilizing local voltage.

VV4 mode, called P control in this paper, does not support any reactive power exchange. Instead, real power output support is limited, or capped, to ensure that the local voltage is kept under the maximum value stipulated by the local grid code.

III. SMART INVERTER SIZING PROBLEM MODELING

For a simple distribution network shown in Figure 2, SI sizing problem is always limited at the edge nodes, i.e. Node 10.

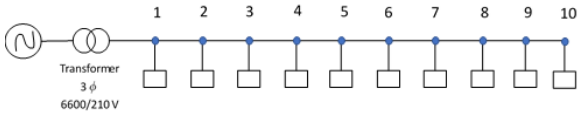

FIGURE 2. A simple distribution network.

Let V_{limit} be the maximum permissible voltage in the network as per the local grid code. Considering that the voltage profile is always most volatile in node 10, it should be ensured that $V_{10} <= V_{limit}$. The voltage rise caused by each inverter can be expressed as (1);

$$V_{increase} = I_{output} * Z_{line} \tag{1}$$

For the sake of simplicity, assume a system where all SIs have the same apparent power output. In this case, the voltage rise at any given $node_i$ can be expressed as:

$$Increase_{node\,i} = V_{increase} * ((n+1) - i) \tag{2}$$

where n represents the number of consecutive nodes in the grid, i.e. for this system 10. It is possible to express the voltage at any $node_i$ as in (3):

$$V_{resultanti} = V_{nominal} + V_{increase}\ \text{x}\ sum_{1->i}(n+1-i) \tag{3}$$

Highest voltage rise occurs at the node that is furthest away from the feeder connection, which is the n^{th} node;

$$V_{nominal} + \left(\frac{n \times (n+1)}{2}\right) * V_{increase} = V_{limit} \tag{4}$$

Normally, grid codes express the maximum allowable voltage as a percentage, g, of nominal voltage;

$$V_{limit} = (100 + g)\%\ \text{of}\ V_{nominal} \tag{5}$$

The overall voltage rise can be expressed as,

$$V_{increase} = \frac{g \times V_{nominal}}{\left(\frac{n\times(n+1)}{2}\right) \times 100} \tag{6}$$

The power flow in an AC system has the well-known equation as in (7).

$$V_{increase} = \frac{RP + XQ}{\hat{V}_s} + j\frac{XP + RQ}{\hat{V}_s} \tag{7}$$

where the sending end voltage, V_s, is expressed as a phasor. If the phasor angles are sufficiently close for sending and receiving end voltages, a simpler version of (7) can be written:

$$V_{increase} = \frac{RP + XQ}{\hat{V}_s} \tag{8}$$

For Figure 2, feeder connection is the most stable node, receiving end, and can be taken as the reference node, i.e. its phasor is set to 0.

$$V_i = V_r + (Rp + XQ) \times \sum_{j=1}^{i} \frac{1}{\hat{V}_j} \tag{9}$$

For n^{th} node, equations (6) and (9) express the same voltage rise:

$$\frac{g \times V_{norminal}}{\left(\frac{n\times(n+1)}{2}\right) \times 100} = (RP + XQ) \times \sum_{j=1}^{n} \frac{1}{\hat{V}_j} \tag{10}$$

Considering that phasor of every node between feeder connection and n^{th} node need to be accounted for, it is not possible to solve this equation in a simple fashion. Furthermore, when SIs operate in volt-var mode, as shown in Figure 1, reactive power becomes a function of voltage, further complicating the situation.

An iterative approach with a powerful simulation tool is the only solution. To this end, a novel power flow simulation tool has been developed which models SI functionalities.

IV. A NOVEL SIMULATION PLATFORM FOR SMART INVERTERS

SoRA-Grid is a novel power flow simulation tool that is geared towards modeling SIs and studying their impact on the power system operation. It has the ability to run both short- and long-term studies ranging from minutes to months. It is a MATLAB-based tool; therefore, models can be developed with Simulink components while profiles such as load and solar radiation, need to be provided as CSV files. SIs can be set to operate in specific modes at specific times.

Traditional power flow approach needs to be customized to account for active components at different nodes. SORA-Grid's power flow iteration follows below steps:

1. *Solve the system with normal Power Flow Iterations*
2. *Solve for V, P and Q values for all nodes*
3. *For nodes where a Transformer, SI or a battery is connected, use these initial V, P, Q values to detect its reaction (e.g. a SI may inject P, or a transformer may change its tap etc.)*
4. *With new values of nodes due to changes in 3, re-run step 1 and 2.*
5. *Repeat above process until the power flow calculations accommodate all SI reactions and a steady-state is reached.*

Obviously, inverters can be set to operate as conventional inverters, no smart functionalities, and the results can be utilized to compare with that of different SI modes. The following section gives the details about the model network, load and solar radiation profiles. Extensive studies are performed with this tool to investigate the impact of SIs on grid operation, optimal PV-INV ratio for SIs and fair use.

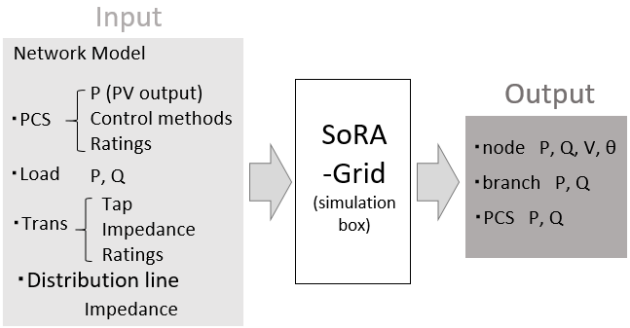

FIGURE 3. SoRA-grid operation.

TABLE 2. Line impedances.

Line No	R[p.u.]	X[p.u.]	Line No.	R[p.u.]	X[p.u.]
1	0	2.8e-4	13	6,02e-3	2.33e-3
2	3.3e-4	3.8e-4	14	05.5e-4	4.8e-4
3	1.8e-4	1.6e-4	15	6.4e-4	5.6e-4
4	7.9e-3	3.05e-3	16	07.4e-4	6.4e-4
5	3.7e-4	3.2e-4	17	9.03e-3	3.5e-3
6	9.3e-4	3.6e-4	18	08.3e-4	7.2e-4
7	9.6e-4	8.4e-4	19	1.62e-3	6.3e-4
8	1.4e-3	1.2e-3	20	2.16e-3	1.88e-3
9	2.5e-3	2.14e-3	21	2.30e-3	2.00e-3
10	2.8e-3	1.08e-3	22	7.87e-3	3.05e-3
11	3.2e-3	1.26e-3	23	03.3e-1	0.19
12	3.9e-3	1.53e-3	24	0.40	0.30

V. DISTRIBUTION NETWORK AND INVERTER MODELING

A. DISTRIBUTION NETWORK MODEL AND ITS PARAMETERS

The simulation system is a typical distribution network as shown in Figure 4. The feeder capacity is 30 MVA. There are 8 commercial loads connected at medium-voltage level (6600 V), and 1404 residential loads connected at low-voltage level (220 V). Figure 5 shows the details of residential nodes where several houses are connected to either side of the pole transformer. In distribution networks with no neutral lines, this topology is utilized to balance the load on both sides of the transformer windings [12]. Industrial loads are connected to only nodes 22, 33, 37, 47, 55, 29, 41 and 51. Being large induction machines, these loads absorb both real and reactive power, P and Q, in contrast to residential load which only absorbs real power, P. In this test, 4 kW PV systems are installed in every house. The PV-INV ratio is defined as the ratio between installed PV array capacity and the inverter capacity. In order to study its impact on system operation and finances, in simulations, this ratio is swept from 50 % to 200 % with 10 % steps. The impedances for electric lines and transformers are detailed in Tables 2 and 3, respectively. Feeder transformer is connected between nodes 2 and 3 while pole transformers are located at each node.

Three nodes are selected for sampling. These are nodes 26, 46 and 59. The motivation behind this is clear. Voltage problems, over voltage or under voltage, are more apparent in the nodes further away from the main grid, i.e. edge nodes. Node 26 is an edge node which is still closer to the feeder connection and is located in high voltage tap zone for the transformers.

Nodes 46 and 59 are edge nodes that are located in the center and ate the end of the distribution network. More importantly, the transformers in this zone use a lower tap setting to account for the voltage drop which is normally observed in passive distribution networks. However, when there is embedded generation, this setting backfires and causes rapid increase in the system voltage due to power injection [13]. For this reason, it is expected that the most

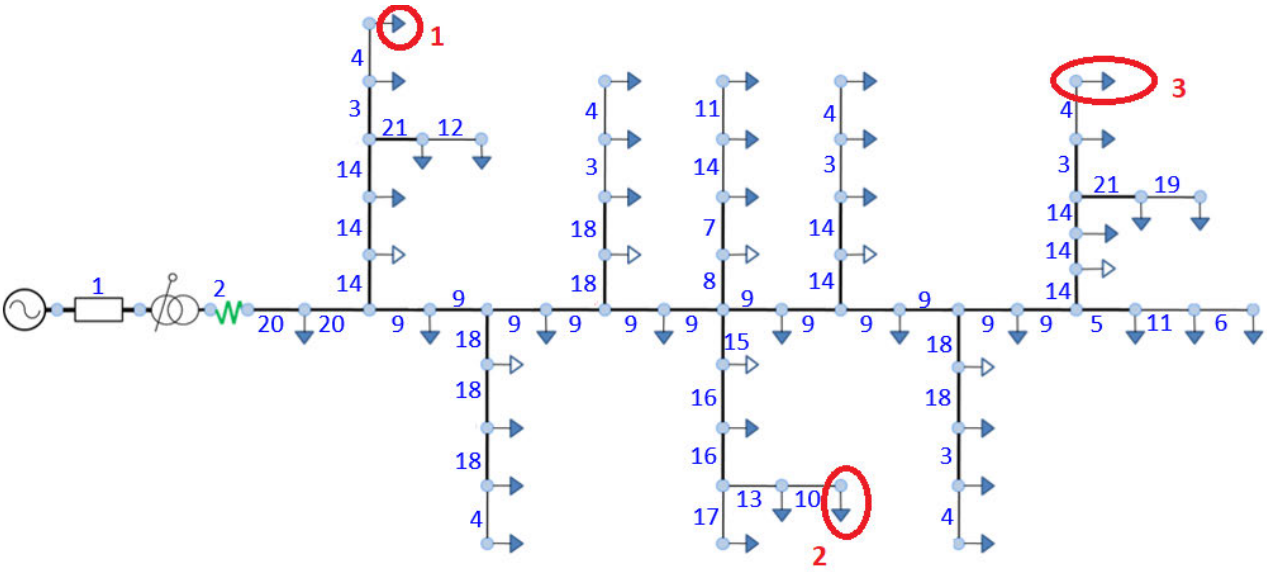

FIGURE 4. Simulated distribution network with corresponding line numbers. Sampled nodes are indicated (1-2-3).

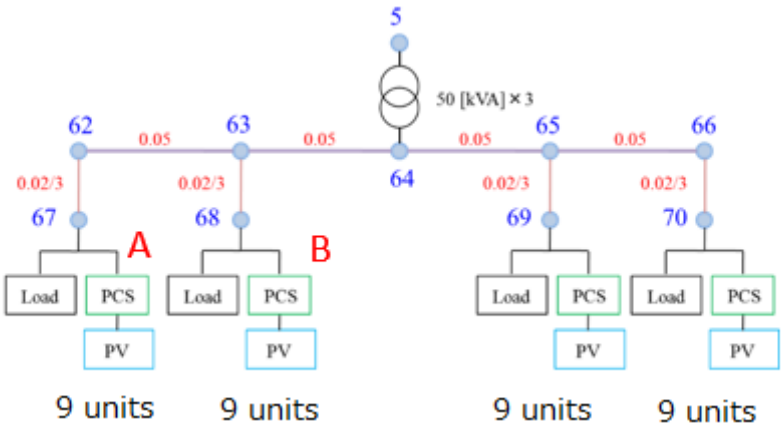

FIGURE 5. Expanded view of connection to pole transformer.

TABLE 3. Transformer parameters.

	Feeder transformer	Pole transformer
Rated capacity [kVA]	30,000	50
Primary Voltage[V]	66,000	6,600
Secondary Voltage[V]	6,600	210
R [p.u.]	0.000822	0.000115
X [p.u.]	0.004932	0.000188

vulnerable is node 59 while other two nodes are sampled for comparison and understanding the magnitude of change.

Figures 6 and 7 show load profiles generated for residential and industrial loads based on a technical report [14]. Profiles are created for weekdays and weekends, and they are multiplied with weight factors to reflect the impact of the seasons. In other words, too cold and too hot seasons have higher factors than mild seasons due to high heating and cooling costs.

B. SOLAR RADIATION DATA AND PV GENERATION

On the other hand, solar radiation profiles are created based on local measurements in FREA's weather station [15]. As shown in Figure 8 and listed in Table 4, this is a well-equipped station where there are nine different measurement devices are located. Pyranometers and spectroradiometers are utilized to measure different types of irradiance. These are utilized for solar radiation estimation and PV module sizing purposes. A windmeter records the speed and direction of wind as FREA has a wind turbine installed on site. Thermos-hygrometer and hyetometer measure temperature, humidity and rainfall to document the characteristics of the local climate.

Equation 11 is utilized to convert local solar radiation measurements to PV generation values

$$E_{PV}(t) = G(t)xP_{PV}\,x\,K \tag{11}$$

where, E is PV generation [kW]; G is irradiance factor which is solar irradiance [kW/m2] divided by standard test condition irradiance, i.e. 1.0 [kW/m2] and Ppv is installed PV capacity which is 4 [kW]. K is PV system coefficient with total inverter efficiency that accounts for several losses including those due to temperature and is taken as 0.85 for this study [15]. This is done for a data that is collected over a full calendar year at one-minute resolution. Figure 9 shows sample generation profiles for each season, i.e. winter, spring, summer and fall. The annual generation is calculated for each inverter for different PV-INV capacity ratios. The load and solar profiles are used for corresponding seasons while smart inverter functionalities are disabled and enabled. Results are compared to see the impact of different smart inverter functionalities on the overall generation and the generated income.

In this simulation, two voltage control methods are used, P control and PQ control. P control reduces active power output when the inverter voltage exceeds the specific upper voltage limit. On the other hand, PQ control, first, supplies reactive power to reduce the voltage rise. If this is not sufficient, then, active power will be capped to voltage below the acceptable limits. It is expected that PQ control will have less active power limitation than P control thanks to its reactive power support.

This is a desirable outcome for the house owners who are installing PV systems. If the active voltage control of the smart inverter results in more active power injection to the grid, this will result in more power being sold to the grid operator, i.e. more profit for the house owner. This will also decrease the payback period for the system.

However, there is an important tradeoff. In P control, the entire inverter capacity is utilized for the active power generation while in PQ control some of this capacity is utilized to exchange reactive power for voltage control purposes. For most cases, this means PQ control would require a larger inverter capacity to be able to control the voltage rise and inject more real power. The voltage control

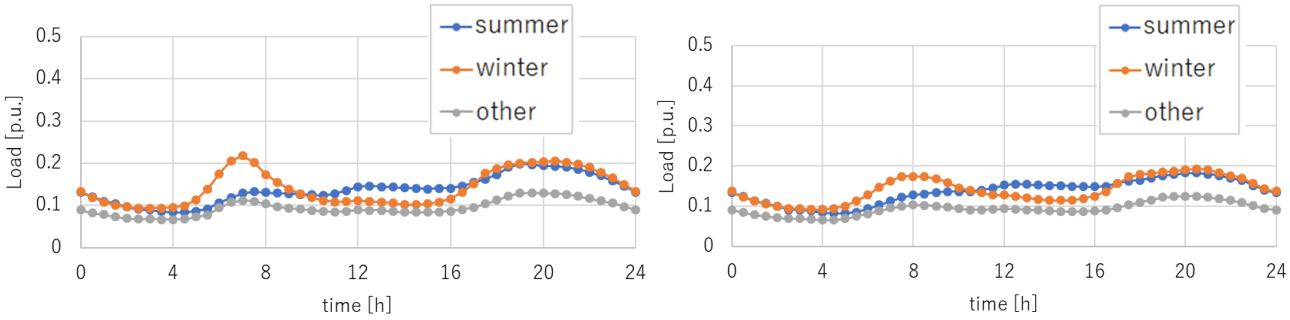

FIGURE 6. Weekday (left) and weekend (right) profiles of residential load.

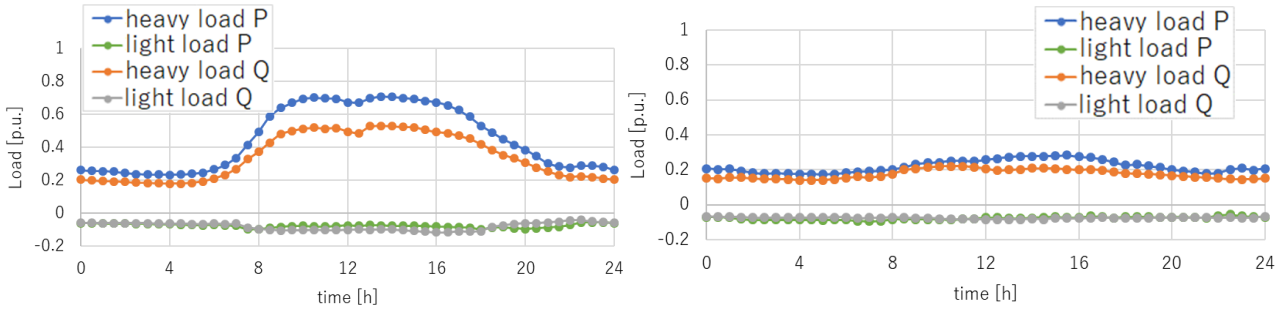

FIGURE 7. Weekday (left) and weekend (right) profiles for industrial load.

FIGURE 8. Local weather station.

TABLE 4. Weather station device list.

	Device	Measurement	Model	Manufacturer
1	Pyranometer	Horizontal Irradiance	CHF-SR20	Hukseflux
2	Pyranometer (tilted 20°)	Slope Irradiance	CHF-SR20	Hukseflux
3	Spectroradiometer [300-1100nm]	Horizontal Spectral Irradiance	MS-711	Eko
4	Spectroradiometer [900-1700nm]	Horizontal Spectral Irradiance	MS-712	Eko
5	Spectroradiometer [300-1100nm]	Direct Spectral Irradiance	MS-711	Eko
6	Pyrheliometer (on the tracker)	Direct Irradiance	CHP 1	Kipp & Zonen
7	Windmeter	Wind speed and direction	CYG-5108	Young
8	Thermo-hygrometer	Air Temp. and Humidity	CVS-HUMICAP180	Vaisala
9	Hyetometer	Rainfall	TKF-1-UD-B	Takeda Keiki

benefit of PQ control comes at a price and this is the increased cost of inverter capacity. While the generated income increases, so does the upfront cost.

On the other hand, for higher capacities, the payback period will be longer for P control as its active power injection capability is directly controlled by the local voltage. PQ control, on the other hand, can utilized its excess capacity to reduce the voltage rise by exchanging reactive power and continue injecting more active power. Therefore, a bigger split is expected between these two control modes at higher PV-INV ratios. Needless to say, in this study, no compensation given to customers for reactive power support. The reactive power support compensation is discussed for future implementation but is not in force yet.

It is true that the physical location of the inverter has a large impact on its operation and the difference between these modes. For instance, nodes that are close to feeder transformer experience much less voltage rise and, thus, need to use much less reactive power exchange. The nodes that are further down are more vulnerable to voltage rise issues and need to utilize more reactive power exchange to be able inject more active power. The fair use of the grid by different customers is a research question in and of itself. In this research, the impact of distance from the feeder on the active power generation ability and smart inverter

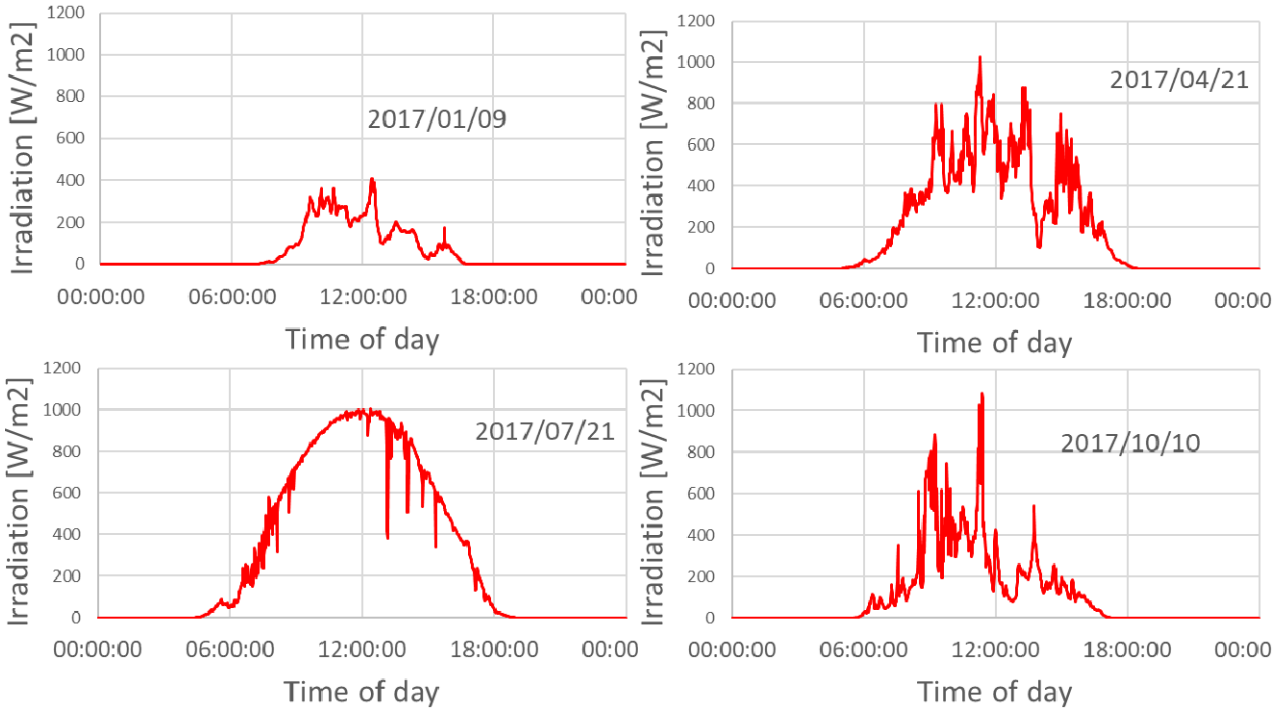

FIGURE 9. Solar radiation profiles for different seasons (clockwise from top left: Winter, Spring, Summer and Fall).

capacity is evaluated. These results can be utilized to develop a fairness scheme where different customers are compensated for different services they provide, such as reactive power exchange to mitigate over voltage issues.

VI. SIMULATION RESULTS AND OPTIMAL PV-INV

The simulations are run with the above conditions for a year. PV-INV ratio is increased from 50 % to 200% with 10% steps. The results are compiled and contrasted to evaluate its impact on overall PV system operation. The evaluation is done in two separate fronts.

Firstly, the annual generation is compared under different conditions. This is important to quantify the impact of different smart inverter methods on overall power generated from the available solar radiation. In the second step, financial considerations are brought in. Two individual factors are utilized to investigate financial performance: payback period and the total profit for 25 years, typical lifetime of a PV system.

A. EVALUATION OF TOTAL ANNUAL GENERATION

Figure 10 shows total annual generation of the entire network for different PV/INV ratios. As expected, overall generation decreases with the PV/INV ratio when the inverter capacity becomes the limiting factor for converting the available solar radiation to electrical energy. P control has 5 % less generation at lower PV/INV ratios. That's because grid voltage reaches the grid code limit (220V in this case). PQ control can mitigate the voltage rise and still continue

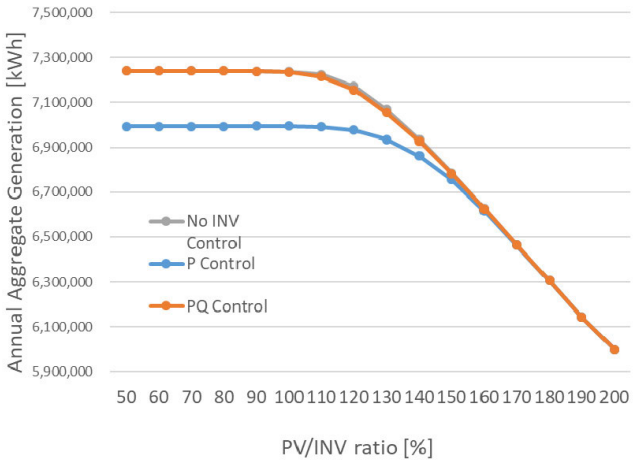

FIGURE 10. Total annual generation vs PV-INV ratio.

inject more active power. The third case, plotted in gray, is where no inverter control is implemented. Inverters keep injecting available power regardless of the terminal voltage levels. This is utilized to compare PQ control with absolute maximum amount of generation available.

As observed, PQ control closely follows no control mode with the exception of 110% to 130% window where it has slightly less generation. As the PV/INV ratio increase, i.e. the inverter capacity decreases, the limiting factor becomes the inverter capacity itself and not the over voltage due to generation. In this case, 160 % ratio, all curves converge

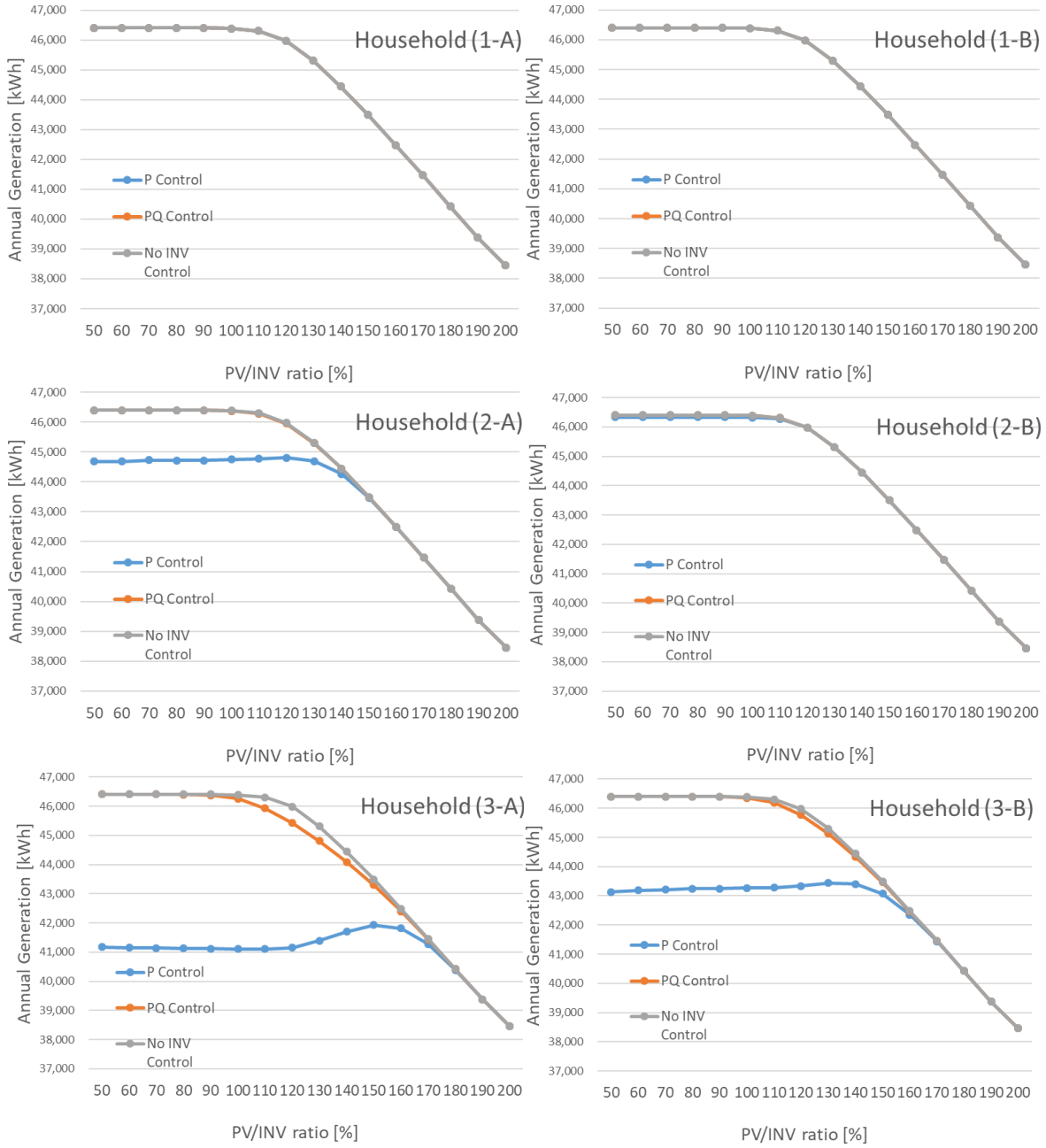

FIGURE 11. **Annual generation per household with different smart inverter controls.**

and generate the energy that fits in the capacity. This is the overall performance of the grid when observed from the feeder connection.

Figure 11 shows individual household connections. Since they are spatially distributed in the grid, the impact of local voltage profile is larger. As shown in Figure 4, the sampling point 1 is the closest to the feeder connection while sampling point 3 is the furthest away, and hence subject to more deviations. Similarly, as shown in Figure 5, household B is closer to the pole transformer as compared to household A. In general, it is observed that the impact of voltage profile become more apparent with increasing distance from the feeder point. Households 1-A and 1-B do not experience over voltage problems. Therefore, their active power generation is never limited, even at 50 % PV/INV ratio. For this reason, all three control modes yield the same amount of energy generation throughout the year. However, in sampling point 2, a change occurs. While household 2-B is much similar to its counterparts in sampling point 1, household 2-A shows that local voltage rises above the permissible limits and P control has to limit its output. This is true for all PV-INV ratios between 50 and 150 %. PQ control has sufficient amount of

extra inverter capacity to counter the local voltage rise and keep its active power generation intact, i.e. as the no control case.

Sampling point 3 is the furthest of them all and shows real impact of voltage profile on smart inverter operation and performance. Both households, A and B, show large impact of unstable voltage profile while the impact is larger in household A. P control shows more than 10 % generation loss between 50 % and 120 % PV-INV ratios. After this, until 170%, decreasing PV/INV ratio avoid over voltage cases.

After this point, inverter capacity dominates as the controlling factor and all three plots converge. The important change in sampling point 3, is that even there is a split between PQ control and no control plots. That's because between 90 % and 160% PV—INV ratios, inverter does not have the sufficient capacity for both active power injection and reactive power exchange. For 2-A and 2-B the voltage rise is not substantial, and the inverter capacity is sufficient to accommodate reactive power exchange to mitigate voltage rise while keeping the real power injection constant. Household 3-A's inverter experiences a much larger voltage rise, therefore, needs to accommodate larger reactive power exchange. Until 80% PV-INV ratio, this can be achieved, but after this point the inverter capacity becomes insufficient to both keep the real power constant and accommodate reactive power exchange to mitigate the voltage rise and keep it within permissible limits.

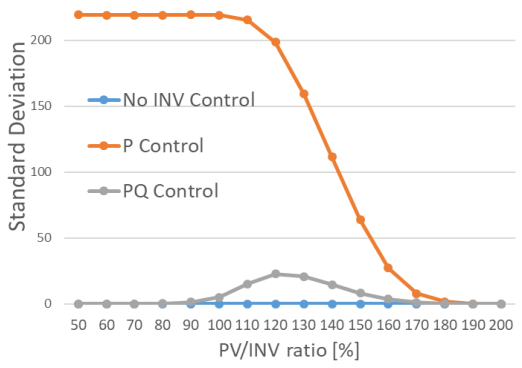

FIGURE 12. Standard deviation of the annual generation of 6 houses.

Figure 12 shows standard deviation between annual generation of six households located in different sampling points. As expected, no control mode yields the same output everywhere. P control has the largest deviation as the injected power experiences more limitation as the node gets further away from the feeder connection point. PQ control has a much smaller deviation, as in certain cases such as household 2-A and 2-B, the inverter capacity is sufficient to mitigate any impact on the real power generation. There are only certain cases where PQ control falls short of voltage control and has to resort to limiting the active generation. Figure 13 shows annual generation per household with PQ control. The deviation occurs in a much smaller window, 90 % to 150 %,

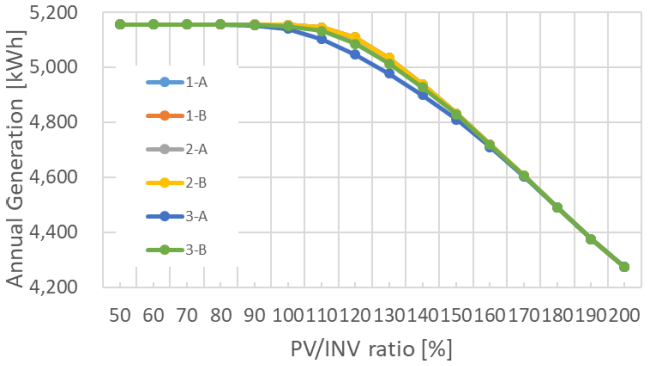

FIGURE 13. Annual generation per PV-INV ratio with PQ control.

and its magnitude is much smaller. This is important in trying to achieve fair operation in distribution networks.

B. ECONOMIC ASSESSMENT OF SIMULATION RESULTS

The results obtained above show that the income generated by PV system is directly related to the PV-INV ratio. In addition to pure technical assessment given above, it is important to consider financial parameters to get a better understanding of the situation. Larger inverter capacity allows for more power generation, hence, income. However, how inverters with larger capacity also cost more. It is important to find the optimal point between these two parameters. Typically, payback period (PP) and total profit (TP) are utilized for economical evaluation of a PV system. These two parameters are calculated for the entire grid, as shown in Figure 14. During these calculations financial values in Table 5 are utilized, which are provided by state authorities [16], [17].

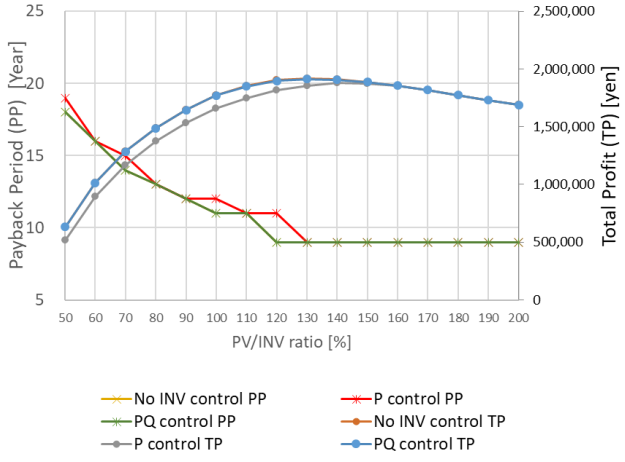

FIGURE 14. Aggregate PP and TP for the grid.

During these calculations equations 12 to 15 are utilized where the parameters are explained in Table 5 below. The overall cash flow is obtained by subtracting reduced electricity bills (Q_{save}) and the profits from energy sales ($E_{surps} * Q_{sell}$) from from overall capital cost (Q_{sys}) and maintenance costs Q_{maint}. The maintenance costs include

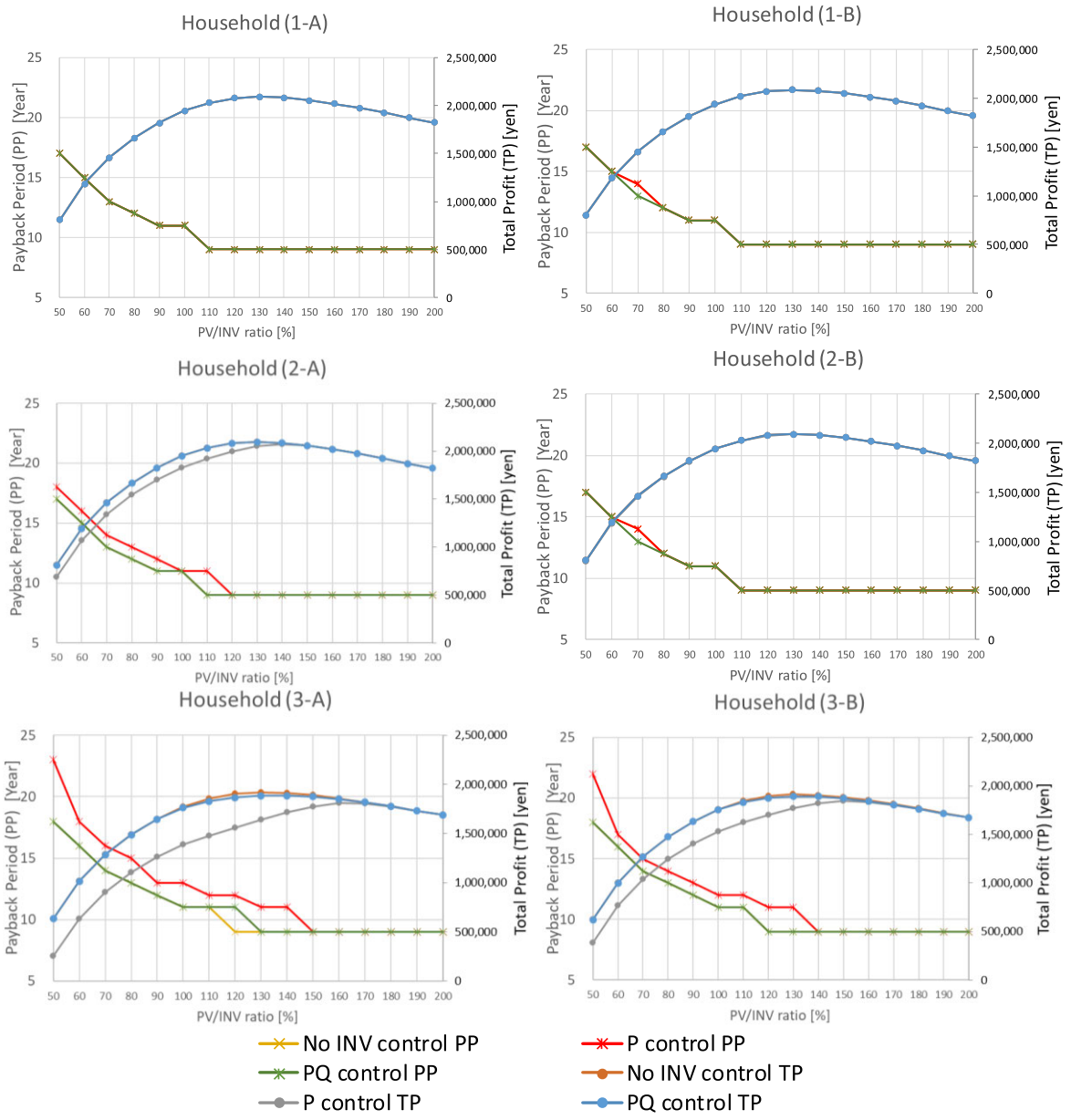

FIGURE 15. Average of PP and TP for sampled houses with different controls.

annual operating costs as well as inverter replacements every L_{INV} years.

$$Q_{CF(y)} = Q_{sys} - (Q_{save} + (E_{surps} * Q_{sell})) - Q_{maint} \quad (12)$$

$$Q_{sys} = (Q_{sys\_PV} * R_{pv}) + Q_{sys\_INV} - Q_{subs} \quad (13)$$

$$Q_{sys\_INV} = Q_{sys\_base} * R_{INV} / 100 * (P_{pv} - P_{INV}) \quad (14)$$

$$Q_{save} = E_{load\_year} * Q_{buy} \quad (15)$$

Overall capital cost is calculated in (3) where PV panel ($Qsys\_PV*Rpv$) and inverter costs $Qsys\_INV$ are added and any subsidies provided by the local governments are subtracted. For instance, in Fukushima prefecture, this is 40,000 yen/kW and it has an upper limit of 160,000 yens [18].

Figure 15 shows PP and TP values for all sampled households. As expected, houses 1-A and 1-B do not show much variation between the control modes. All PP and TP values are almost the same as no control mode. When the PV-INV ratio is too high, the inverter is small and not much energy is generated. Therefore, the TP is small, and PP is high. As the PV-INV ratio decreases, the amount of generated energy increases, raising TP and decreasing PP. At 130% TP curve peaks, because the all of the available solar energy is converted to electricity with this capacity. Any increase in PV-INV ratio would result in higher inverter capacity that is not needed. This increases the capital costs and maintenance costs, driving PP to very high values.

TABLE 5. Parameters for calculating cash flow.

Income Parameters		
Q_{sell}	*Electricity selling price [yen/ year]*	*26*
E_{surps}	*Annual Inverter output power to selling grid[kWh/year]*	*variable*
E_{load_year}	*Annual Inverter output power to supply own load[kWh/year]*	*variable*
Expense Parameters		
Purchase of electricity from systems		
Q_{buy}	*Electricity Price [yen/kWh]*	*28.75*
System installation and maintenance costs		
Q_{sys}	*Equipment cost [10,000yen/kW]*	*36.4*
R_{PV}	*Rate of PV cost in Q_{sys} [%]*	*52*
R_{INV}	*Rate of SI cost in Q_{sys} [%]*	*11*
L_{INV}	*Lifetime of Inverter [year]*	*10*
Q_{maint}	*Maintenance cost [yen/kW/year]*	*1,200*

In houses 3-A and 3-B, the difference between P control and PQ control becomes more apparent. For 3-A, the TP starts shooting down at 170% ratio as anything after that would cause over-voltage issues in the grid and the PV system cannot inject anymore energy, no matter how much solar radiation is available or the capacity of the inverter. PQ control, on the other hand, keeps increasing TP with decreasing ratio (i.e. increasing inverter capacity), as some portion of increased capacity is utilized for reactive power exchange. Hence, more real power can be generated and injected to the grid. The results show that P control may have 33 % longer PP and may generate 60% TP. The average TP and PP for the sampled houses are given in Figure 16.

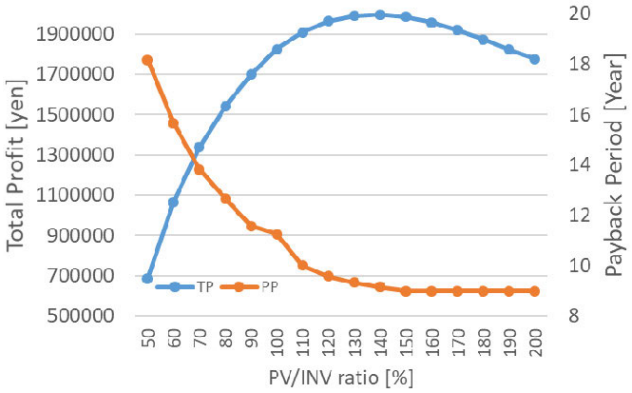

FIGURE 16. Average of PP and TP for samples houses.

Figure 16 shows the average PP and TP for both P control and the PQ control. From financial viewpoint, short PPs and high TPs are desirable. Since these two parameters play a major role in ratio selection, a combine approach is required. TP and PP are normalized as in equations 16 and 17, where TP_{nom} normalized total profit, TP_{min} and TP_{max} are minimum and maximum total profits belonging to smart inverters deployed in the simulated network. Similarly, PP_{nom} is normalized payback period PP_{min} and PP_{max} are minimum

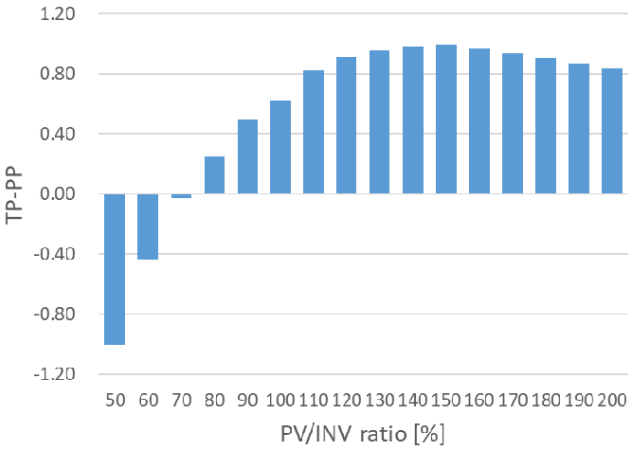

FIGURE 17. Difference of normalized both TP and PP.

and maximum payback periods found for smart inverters deployed in the simulated network.

$$TP_{nom(i)} = (TP_{(i)} - TP_{min})/(TP_{max} - TP_{min}) \quad (16)$$

$$PP_{nom(i)} = (PP_{(i)} - PP_{min})/(PP_{max} - PP_{min}) \quad (17)$$

This way they can be used as a scalar parameter of same magnitude. The difference, D_i, shown in equation 18, is plotted as in Figure 17.

$$D_{(i)} = MAX(TP_{nom} - PP_{nom}) \quad (18)$$

As shown, for average values TP and PP the most optimal value turns out to be 150% that gives the highest TP with shortest PP. These values can be utilized by the grid operators as standard values for any PV system to be installed in the network. Thus, all house owners would get a fair use of the grid.

VII. CONCLUSIONS

Smart Inverters are becoming more popular thanks to their advanced capabilities. They can support the grid voltage and frequency. Of these, the voltage control is especially valuable for PV systems connected to low voltage networks. These networks tend to see more substantial voltage rises and smart inverter voltage support may be utilized to prevent these events. However, the optimal capacity for supporting the grid while injecting real power needs to be investigated.

In this paper, a thorough study is performed to find this optimum capacity. Extensive simulations studies are performed to calculate overall generation of PV systems. Solar radiations based on real measurements are used to calculate PV generation while realistic profiles are used for loads. A new simulation tool is developed to integrate smart inverters modes into the power flow studies. The results show that nodes that are further away from the feeder connection point are more vulnerable to voltage variations and, thus, may benefit more from smart inverter functions. The impact on overall payback period and total profit can be substantial when different functions are utilized. The results can be used

to enforce a uniform PV-INV ratio across the network to achieve a fairer use of the grid infrastructure

These results are useful for electric power companies, house owners and policymakers. The impact of SI location, its size and different operating modes are quantified. The location may reduce the overall generation more than 10 % and may decrease overall profit by 40 %. This means, the owners may be looking at 33 % longer payback times. Considering that smart inverters provide auxiliary grid support and everyone should have the equal right to access and use power infrastructure, fair operation rules need to be developed. One way is to compensate smart inverter owners for the auxiliary support. The other option is to enforce a fixed inverter size all over the grid as shown in this paper.

REFERENCES

[1] *REthinking Energy 2017: Accelerating the Global Energy Transformation*, Int. Renew. Energy Agency, Abu Dhabi, United Arab Emirates, 2017.

[2] *The Rise of Renewable Energy and Fall of Nuclear Power, Competition of Low Carbon Technologies*, Renew. Energy Inst., Tokyo, Japan, 2019, p. 80.

[3] A. H. Hubble and T. S. Ustun, "Scaling renewable energy based microgrids in underserved communities: Latin America, South Asia, and Sub-Saharan Africa," in *Proc. IEEE PES PowerAfrica*, Livingstone, Zambia, Jun. 2016, pp. 134–138.

[4] A. H. Hubble and T. S. Ustun, "Composition, placement, and economics of rural microgrids for ensuring sustainable development," *Sustain. Energy, Grids Netw.*, vol. 13, pp. 1–18, Mar. 2018.

[5] *Communication Networks and Systems for Power Utility Automation, Part 90-7: Object Models for Power Converters in Distributed Energy Resources (DER) Systems*, Standard IEC/TR 61850-90-7, International Electrotechnical Commission, Feb. 2013.

[6] J. Hashimoto, T. S. Ustun, and K. Otani, "Smart inverter functionality testing for battery energy storage systems," *Smart Grid Renew. Energy*, vol. 8, no. 11, pp. 337–350, 2017, doi: 10.4236/sgre.2017.811022.

[7] T. S. Ustun and S. Mekhilef, "Design and implementation of static synchronous series compensator with a soft-switching H-bridge inverter with DSP-based synchronization control," *Int. Rev. Electr. Eng.*, vol. 5 no. 4, pp. 1347–1353, 2010.

[8] T. S. Ustun and Y. Aoto, "Analysis of smart inverter's impact on the distribution network operation," *IEEE Access*, vol. 7, pp. 9790–9804, 2019, doi: 10.1109/ACCESS.2019.2891241.

[9] T. M. Wanzeler, J. P. A. Vieira, P. Radatz, V. C. Souza, and D. C. Pinheiro, "Assessing the performance of smart inverter volt-watt and volt-var functions in distribution systems with high PV penetration," in *Proc. Simposio Brasileiro Sistemas Eletricos (SBSE)*, Niterói, Brazil, May 2018, pp. 1–6.

[10] A. Del Pizzo, L. P. Di Noia, and S. Meo, "Super twisting sliding mode control of smart-inverters grid-connected for PV applications," in *Proc. IEEE 6th Int. Conf. Renew. Energy Res. Appl. (ICRERA)*, San Diego, CA, USA, Nov. 2017, pp. 793–796.

[11] M. S. Hossan, V. Westfallen, E. A. Paaso, M. Avendano, and S. Bahramirad, "Usage of smart inverter Q-V droop functionality for irradiance variation induced voltage fluctuation reduction considering system uncertainty," in *Proc. IEEE Power Energy Soc. Innov. Smart Grid Technol. Conf. (ISGT)*, Washington, DC, USA, Feb. 2018, pp. 1–5.

[12] Institute of Electrical Engineers of Japan. *Japanese Power System Models*. Accessed: Aug. 28, 2019. [Online]. Available: http://denki.iee.jp/pes/?page_id=141

[13] *Overcoming Urban Power Distribution Challenges With Technological Innovations*, ABB Automat. Power World Mag., Special Ed., Feb. 2015.

[14] *Power Factor Issue on Distribution Network: Appendix 5, Average Load Curve of High Voltage Distribution Line*, Electr. Technol. Res. Assoc., (in Japanese), vols. 1–66, 2010, pp. 97–103.

[15] T. S. Ustun, Y. Nakamura, J. Hashimoto, and K. Otani, "Performance analysis of PV panels based on different technologies after two years of outdoor exposure in Fukushima, Japan," *Renew. Energy*, vol. 136, pp. 159–178, Jun. 2019.

[16] *Transport and Industry, Recent Trends in Solar PV Market*, (in Japanese), Ministry Energy, New Delhi, India, 2014.

[17] *Transport and Industry, Procurement Prices for 2015 Fiscal Year*, (in Japanese), Ministry Energy, New Delhi, India, 2015.

[18] *Fukushima Renewable Energy Promotion Center, Homepage*, (in Japanese), Renew. Energy Promotion Center, Fukushima, Japan, 2018. [Online]. Available: https://fukushima-pv-hojo.org

TAHA SELIM USTUN (Member, IEEE) received the Ph.D. degree in electrical engineering from Victoria University, Melbourne, VIC, Australia. He was a Faculty Member with the School of Electrical and Computer Engineering, Carnegie Mellon University, Pittsburgh, PA, USA. He is currently a Researcher with the Fukushima Renewable Energy Institute, AIST (FREA), where he leads the Smart Grid Cybersecurity Laboratory. His current research interests include power systems protection, communication in power networks, distributed generation, microgrids, electric vehicle integration, and cybersecurity in smart grids. He is a member of the IEEE 2004 and 2800 IEC Renewable Energy Management WG 8 and IEC TC 57 WG17. He has been invited to run specialist courses in Africa, India, and China. He has delivered talks for the Qatar Foundation, the World Energy Council, the Waterloo Global Science Initiative, and the European Union Energy Initiative (EUEI). His research has attracted funding from prestigious programs in Japan, Australia, EU, and North America. He serves on the Editorial Board of the IEEE Access, the IEEE Transaction on Industrial Informatics, Energies, Electronics, Electricity, and the *World Electric Vehicle and Information* journals.

YUKI AOTO graduated from Tokyo Kasei Gakuin Tsukuba Women's University, in 2001. She has been working as a Programming Specialist with the Energy Network Team of the Renewable Energy Research Center, Fukushima Renewable Energy Institute, AIST, since 2015.

JUN HASHIMOTO has contributed to PV research, especially PV system performance testing and characterization, since joining AIST, in 2017. More recently, he has expanded his research to study smart grid systems, especially advanced inverter interoperability for PV and energy storage. He is currently involved in IEC TC82 WG2, 3, 6, and 7 to develop international standards as an expert on PV modules, systems, and CPV.

KENJI OTANI currently leads the Energy Network Team of the Renewable Energy Research Center, Fukushima Renewable Energy Institute, AIST. He has researched the system integration technologies of PV and hybrid power systems.